ФИЗИКА ЭЛЕМЕНТАРНЫХ ЧАСТИЦ И АТОМНОГО ЯДРА
2013. Т. 44. ВЫП. 4

FIRST SAMPLES OF Ti AND Nb TUBES EXPLOSION WELDING JOINT WITH STAINLESS STEEL FOR ILC 1.8 K CRYOMODULE

B. M. Sabirov, J. A. Budagov, G. D. Shirkov

Joint Institute for Nuclear Research, Dubna

ФИЗИКА ЭЛЕМЕНТАРНЫХ ЧАСТИЦ И АТОМНОГО ЯДРА
2013. Т. 44. ВЫП. 4

FIRST SAMPLES OF Ti AND Nb TUBES EXPLOSION WELDING JOINT WITH STAINLESS STEEL FOR ILC 1.8 K CRYOMODULE

B. M. Sabirov, J. A. Budagov, G. D. Shirkov

Joint Institute for Nuclear Research, Dubna

The world first samples of Ti and Nb tubes joint with stainless steel ones by an explosion welding were manufactured in the frame of ILC R&D program by the JINR–VNIIEF–FNAL–INFN cooperation.

An applying of methods of relaxation of residual tensions (after explosion and electron beam welding), macro- and microanalyses of welding seam, and cryogenic tests of the samples produced manifest the achievement of high mechanic strength ($\approx$ 250 MPa/share) of welding seam, solidity and leak absence on 10^{-10} l $\cdot$ atm/s level at 1.8 K.

The explosion welding technology and methods introducing to industrial manufacturing of the 4th generation of cryomodule of TESLA TYPE DESIGN can exclude the Ti communications, connect the Nb cavity with stainless steel vessel and reduce significantly the accelerator cost.

В рамках сотрудничества ОИЯИ–ВНИИЭФ–FNAL–INFN впервые в мире созданы трубчатые соединения Ti и Nb с нержавеющей сталью методом сварки взрывом.

Применение методов релаксации остаточных напряжений после сварки взрывом и электронно-лучевой сварки, макро- и микроанализ сварных швов и криогенные исследования изделий свидетельствуют о достижении высокой механической прочности ($\approx$ 250 МПа на срез) сварных швов, плотности и отсутствии течи на уровне 10^{-10} л $\cdot$ атм/с при температуре 1,8 K.

Внедрение созданных технологий и методов сварки взрывом в промышленность для создания криомодулей 4-го поколения (TESLA TYPE DESIGN) позволит исключить Ti-коммуникации, соединить Nb-резонатор с нержавеющей сталью оболочки криостата и существенно понизить стоимость ускорителя.

PACS: 41.75.Ht; M81.05.-t; 07.20.Mc; 07.30.Hd; 07.85.Jy

INTRODUCTION

In the year of 2001 there began the construction of a Large Hadron Collider (LHC) in CERN. The LHC has been steadily operating since November of 2009, and by the dawn of 2012, for the first time in the history of high energy physics, the energy of protons had been increased up to the record value from 2 to 3.5 TeV, and the peak of luminosity reached $5 \cdot 10^{32}$ cm$^{-2} \cdot$ s^{-1}. At present, the LHC is considered to be the largest experimental facility in the world; the length of the basic accelerator circumference is as long as 26 659 m.

Along with the creation and the launch of the LHC, the leading laboratories of the world were working over development of a next-generation accelerator — electron–positron collider, which was meant to require total energy of up to 1 TeV and even higher. While electrons and positrons run round the circular orbits at such energies, the loss of their emission becomes so great that the energy of particles is hardly possible to fully refill by accelerating structures and the circular accelerator itself or collider becomes technically difficult to operate. This explains why at present the electron–positron colliders of the future are considered to be linear accelerators.

Premier developments of electron–positron linear colliders of high energies began as early as in 60s–70s of the XX century in large scientific centers such as CERN, SLAC, DESY, KEK, Budker INP, Kharkov IPT. By the beginning of 2000 there were three most advanced projects like Next Linear Collider (NLC) in SLAC (USA), Linear Collider (JLC) in KEK (Japan), and TeV Energy Superconducting Linear Accelerator (TESLA) in DESY (Germany).

The technology of superconducting accelerating systems based on niobium cavities had been developing in DESY since 1992. These developments resulted in appearance of a number of projects including Free-Electron Laser in Hamburg (FLASH), X Free Electron Laser (XFEL) and electron–positron collider TESLA. In 2001, there was prepared the Technical Design Report on TESLA Project, which assumed the building of a linear electron–positron collider with the centre-of-mass energies up to 500 GeV, which in its turn might be further increased up to 800 GeV. The collider was supposed to be built in eight years in the German accelerator centre DESY nearby Hamburg. The length of the TESLA linear accelerator should have been of about 33 km.

The zest of the TESLA Project compared to the competitive projects of linear colliders was the simultaneous creation of X Free Electron Laser (XFEL) with high luminosity. Besides, unlike NLC and JLC, the TESLA Project used 21024 special superconducting accelerating cavities at the frequency of 1.3 Hz, which were maintained at the temperature of $-271\,^{\circ}$C. Superconducting cavities create an accelerating gradient exceeding 25 MV/m, which allows one to aim at colliding lepton energy of 500 GeV at a given length of the collider. At present, it has been possible to obtain an accelerating gradient up to 50 MV/m on separate cavity specimen of this type under laboratory conditions. SLAC and KEK presented the projects of colliders with «warm» linear accelerators working at frequencies of 11.4 GGz.

At the dawn of 2003, the government of Germany made a decision to create European X-ray Laser Project (XFEL) separately from TESLA. In 2004, the XFEL Project was supported and approved by the European Committee. Besides, in DESY the FLASH Project was successfully implemented, which at present is the most perfect laser on free electrons in the field of vacuum ultraviolet and soft X radiation. At the same time, the full TESLA Project was indefinitely adjourned.

At present, the XFEL Project is at the stage of implementation. The tunnel of 3.4 km was built in the DESY neighborhood nearby Hamburg. The construction works are in full swing and the serial production of superconducting accelerating modules has begun. According to the schedule in 2015, it is planned to obtain the electron beam with the energy of 17.5 GeV, and the final full launch of the whole facility is planned in the year of 2016. Russia is taking the most active part in XFEL Project, having invested about 300 million euros into its creation (about 30% of the whole cost of the Project).

At the dawn of 2000, the scientists of a number of Asian countries published the project of Global Linear Collider GLC. It was based on the use of warm accelerating structures working at the frequency of 11.4 GeV. However, in 2004 the International Advisory Board on technology of accelerators suggested that the project of this collider should be changed by means of superconducting technology using superconducting accelerating TESLA modules, which had already been developed and verified in DESY. With this in view, the International Committee for Future Accelerators (ICFA) of the International Union of Pure and Applied Physics (IUPAP) declared about the most important decision to unite the efforts of scientific centers of the world in creation of accelerating complex of the next-generation electron–positron linear collider. This unique project was named International Linear Collider (ILC). Thus, three existing NLC, GLC, and TESLA Projects were joined into one ILC Project.

Along with the ILC Project, the development of a two-beam compact electron–positron collider CLIC based on «warm» technologies has been carrying out in CERN for a long time. This accelerator is supposed to have the rate of acceleration of up to 100 MV/m which will allow the total energy of colliding particles three times as high at the same length of the accelerator. However, as of this time, the research using this method has not been completed yet, and at present, the experimental works on CLIC collider are carried out at the research test stand CTF3 in CERN. The tests of all the systems and experimental verification of the two-beam technology of CLIC are supposed to be completed with the preparation of the TDR collider technical project by the year of 2016.

By the decision of ICFA, in the summer of 2012 there was created a unified Linear Collider Board LCB in order to coordinate all the works on future linear colliders.

The conceptual ILC Project (RDR — Reference Design Report) was implemented in 2006 and presented at the session of ICFA Committee in February of 2007 in Beijing. According to this document, the nominal luminosity (full intensity of interaction at the point where beams collide) at the particles' energy of 500 GeV amounts to $2 \cdot 10^{34}$ $\mathrm{cm^{-2} \cdot s^{-1}}$. The energy of 500 GeV at the facility based on TESLA cavities can be obtained if the rate of acceleration of all 20000 cavities will be 31.5 MV/m, and the length of each of the two linear colliders will be as long as 11 km. With the further increase of the energy up to 1 TeV the rate of acceleration of the cavities should be 36 MV/m, which would require the increase of the length of each of the two linear accelerators by 9.3 km. In this case the full length of the two linear accelerators will make about 40 km, and the length of the whole facility (full length of the tunnel) would be about 50 km. In the years of 2005–2006 five research centers, which submitted applications, are officially considered to be the probable candidates for placement of ILC in their countries: CERN (Switzerland, France); DESY (Germany); E. Fermy Laboratory (USA); KEK Laboratory (Japan); JINR (Dubna, Russia). By the end of 2012 there will have been prepared the TDR ILC Technical Project.

According to the decisions of the Scientific Council and the JINR Plenipotentiary Committee, JINR began the works on the ILC Project in 2005. Dubna city was suggested as the place for location of a new collider. At the same time, several JINR research groups are taking part in the developments connected with the CLIC Project in CERN. The research on LHC Project was initiated by Academician A. N. Sissakian, and at present, it is widely carried out in several directions. One of these directions is introduced in this paper.

Construction of the new accelerator is expected to favor development of promising directions in nuclear power and technology researches and, as a consequence, to contribute to investigations of new power sources, new materials, new technologies, etc. Apart from the leading physics research centers in the United States, Japan, Germany, and Russia (JINR) aspiring to accommodate the ILC on their territory, there is a great deal of other research centers in many countries that participate in the project.

At the first stage, the collider is supposed to accelerate electron–positron beams to the energy of 0.5 TeV; the total length of the accelerating section is about 35 km (Fig. 1).

To accelerate electrons and positrons over this length, superconducting cavities of highly pure niobium (Nb) with the working strength of the accelerating

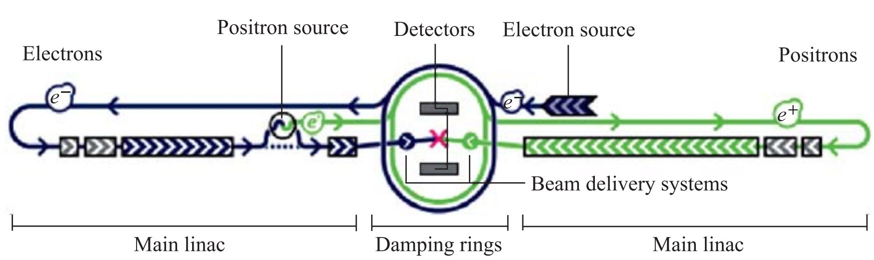

Fig. 1. Schematic view of the ILC

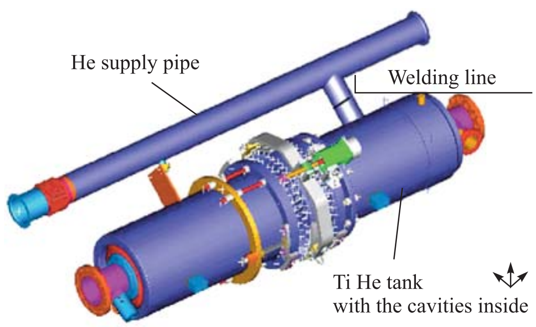

Fig. 2. A way of joining the helium supply pipe and the titanium tank with a niobium cavity inside

field up to 35 million volts per meter at the radio frequency 1.3 GHz are used. A total of 20 000 cavities like this are needed. The cavities must be kept at the temperature 1.8 K. To this end, they are placed in titanium (Ti) cryostats with liquid helium. A helium supply pipe of titanium is laid along the entire accelerator length for continuous supply of helium to the cryostats. Titanium (Ti) was chosen for the specific welding properties of niobium and titanium and for the minimal residual magnetism of these materials.

JINR, FNAL, and INFN (Pisa) investigated the possibility of making the helium supply pipe from stainless steel (SS), which promises an appreciable decrease in the cost of the project. The problem in this option is the joining of the stainless-steel pipe and the titanium tank (Fig. 2).

Participation of the Russian Federal Nuclear Center — Institute of Experimental Physics (RFNC–VNIIEF, Sarov) resulted in a fundamentally important solution of the problem: explosion welding allowed joining not only titanium and stainless steel but also niobium and stainless steel. This achievement opens up a unique possibility of developing a new design of the IV generation cryomodule, which can lead to a radical reduction in the cost of the ILC due to substitution of SS for Ti. This review sums up the results of R&D carried out by the JINR–VNIIEF–FNAL–INFN collaboration in this field.

1. Ti–SS TREATMENT

1.1. Development of the Procedure for Explosion Welding of Coaxial Bimetallic Joints. As is known, SS and Ti cannot be welded by the conventional methods of electron-beam or electric-arc welding. To solve the problem of joining the helium supply pipe of stainless steel and the titanium tank, a group from

KEK (Japan) tried to weld SS and Ti tubes using two unconventional methods of friction welding and isostatic hot pressure welding [1]. The pieces were in general welded, but the weld turned out to be as brittle as ceramic, which was unsuitable for operation at ultralow temperatures. A more reliable method was needed. This method is available at VNIIEF (Sarov).

Dubna and Sarov have been bound by scientific relations in many research fields for many years. These relations further continued in the scope of the ILC project [5]. A unique welding method proposed in Sarov uses the explosion energy. Generally speaking, explosion welding of two different metals is known and well studied in the world, but it was used to weld flat pieces [2, 3]. In Sarov, on the initiative of JINR, a unique method of welding coaxial pieces was developed and practically used [4, 5].

Explosion welding (EW) experiments were set up to attain the following technological objectives:

— to develop the optimum design for a tubular bimetallic transition element,

— to optimize dimensions of a bimetallic billet for the transition element,

— to design initial billets and auxiliary equipment for explosion welding,

— to find the appropriate explosion welding scheme,

— to choose technological parameters of explosion welding,

— to design equipment for leakage tests.

After the above objectives were attained, an experimental investigation was carried out to determine the optimum technological parameters of explosion welding by the parallel welding scheme (Fig. 3) using the Russian materials, 12X18H10T steel (analogue of 321 steel) and BT1-0 titanium (see Appendices).

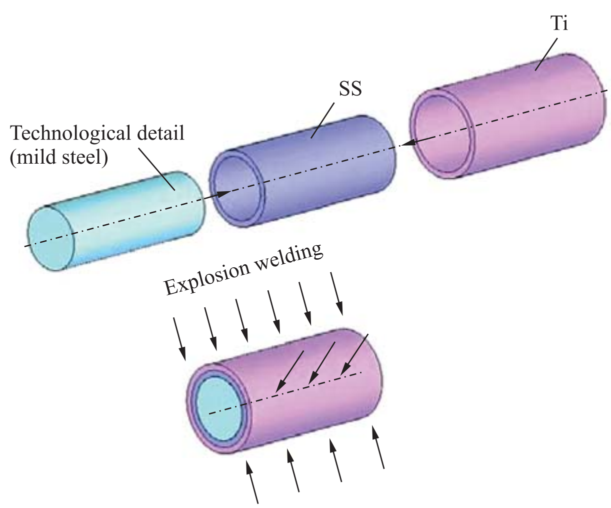

Fig. 3. Parallel welding scheme

The resulting specimen was subjected to a primary leakage tested and to metallographic investigations in Sarov. The second specimen was made, and samples were cut from it along the weld. The metallographic investigation of the welded joint included

— macroanalysis,

— microanalysis,

— measurement of microhardness.

Macroanalysis of the welded joints was carried out to reveal possible macrodefects (cracks, poor penetration, separation into layers) and determine parameters of the wave at the titanium–stainless steel interface (shape, length, amplitude).

Microanalysis was carried out to examine the microstructure of the welded materials in the welded joint area and reveal possible microdefects (intermetallide compounds, microimperfections).

Measurement of *microhardness* was performed to determine changes in mechanical properties of the materials in the welded joint area.

The metallographic investigation revealed no macrodefects of welded joints like cracks, poor penetration, and separation into layers. The welded joint of BT1-0 titanium and 12X18H10T steel shows a wave-like nature, which contributes to its strength. The «waves» formed during the explosion welding have a nearly sinusoidal shape. The lengths and amplitudes of the waves in both samples are identical, being $\cong 0.3$ and $\cong 0.05$ mm, respectively (Fig. 4).

During the explosion welding, plastic deformation of welded materials occurs in the contact surface area. Evidence for a high degree of plastic deformation of BT1-0 titanium and 12X18H10T steel is a large number of twins in their structure (Fig. 5).

During the explosion welding of BT1-0 titanium and 12X18H10T steel, individual microdefects like microimperfections and intermetallide phases were formed. In the investigated samples, the microdefects are local and do not form a continuous patch, which in no way affects the strength of the joint and the density of the weld.

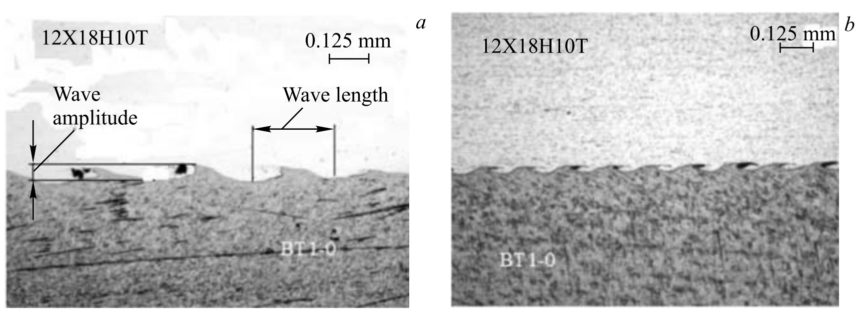

Fig. 4. Macrostructure of the BT1-0 titanium–12X18H10T steel welded joint

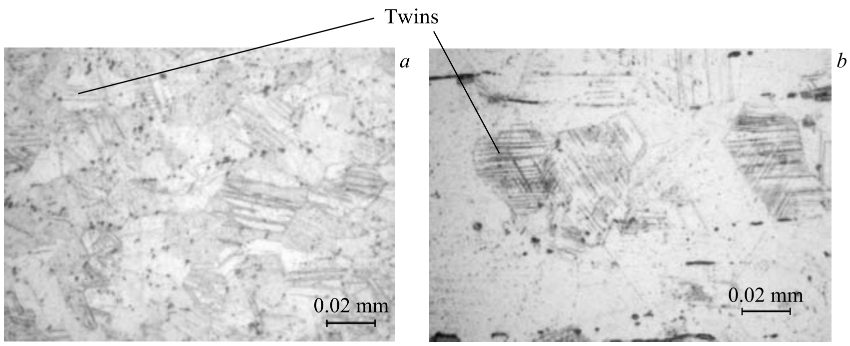

Fig. 5. Microstructure of BT1-0 titanium (a) and 12X18H10T steel (b) in the welded joint area

During the explosion welding of titanium and steel, metal strengthening due to shock compression is observed in the welded joint area. Microhardness measurement was performed to determine changes in mechanical properties of the materials in the welded joint area. The microhardness measurement method [4] consists in that a regular four-sided diamond pyramid with a square base and a vertex angle of 136° is pressed under a certain load P into the surface under investigation and kept in this position for 15 to 20 min. Then the load is removed from the pyramid and there remains an imprint in the surface under investigation (Fig. 6). Its diagonals are measured and their average value (d) is then calculated.

Microhardness HV is calculated as a quotient of dividing the load by a conventional area of the side surface of the imprint F

$$\mathrm{HV} = \frac{P}{F}, \quad \text{where} \quad F = \frac{d^2}{1.8544}.$$

Microhardness was measured using the PMT-3 instrument. The strengthening of the material is most intensive in a narrow zone near the BT1-0 titanium–

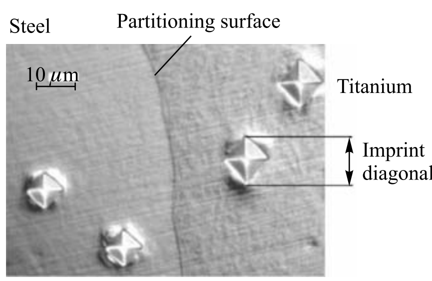

Fig. 6. Imprints on the surface under investigation after the microhardness measurement in the titanium–steel weld area

12X18H10T steel interface (Fig. 7). In each material, the width of this zone is ≈ 0.5 mm. The farther away from the interface, the less the metal strengthening. The strengthening arising in the area of the welded joint increases the strength of the metals but decreases their ductility.

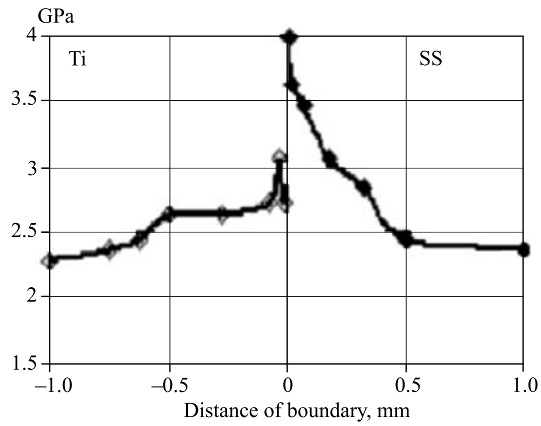

Fig. 7. Microhardness distribution around the explosion welding line

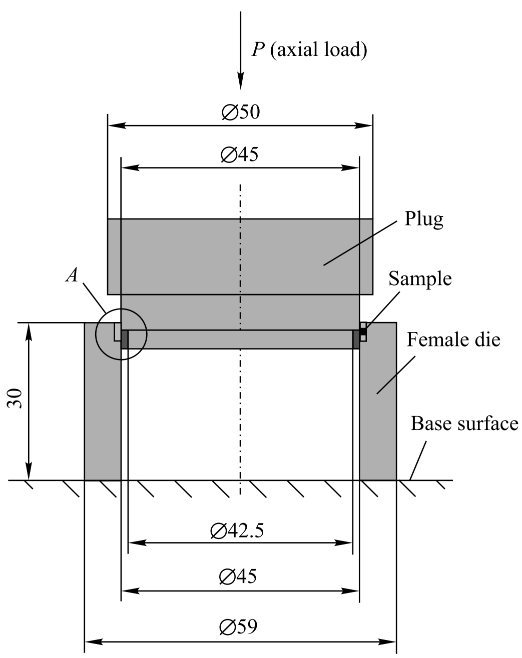

Fig. 8. Schematic view of a setup for testing the Ti–SS sample for shear

The shear strength of the welded joint was measured [4]. Special equipment and a ring of appropriate configuration were made to produce pressure on the titanium part by a mechanical press until shear occurs (Fig. 8).

The result turned out to be quite impressive: $\tau_{\mathrm{sh}} \cong 250$ MPa. The leak test of the welded joint in Sarov was carried out using the PTI instrument (helium leak detector). The samples were tested at room temperature and after being cooled by liquid nitrogen for ≈ 10 min. The test showed that all tested samples were leak proof: no leak occurred at the background leak rate 10^9 atm · cc/s according to the PTI [4].

Thus, the mechanical and metallographic investigations and the leak measurement carried out in Sarov proved that (i) explosion welding provided bonding of titanium and stainless steel cylinders, and (ii) the welded joints showed the necessary level of strength and density.

1.2. Development, Making, and Test of a Bimetallic Tube Sample Similar in Design to the Working Version of the Cryomodule. The next step was a change-over from the parallel welding of pipes to the butt welding of the Ti and SS pieces, which allows the bimetallic element to be used in the cryomodule. Yet, in the course of solving this problem, the parallel welding scheme was used again. A schematic view of this tube sample is shown in Fig. 10, as well as the developed scheme of this tube model. The titanium and stainless steel components are set butt to butt and explosion-welded by the parallel scheme using a stainless steel coupling. It is worth noting that according to the cryomodule specification, only 316L austenitic steel should be used; moreover, it should be of EN 1.4429 (316LN) modification, which, as is evident from the plot (Fig. 9), has a minimum admixture of the ferrite component ($< 5\%$) and no martensite component at all [17]. Since our objective was to develop a production technology and design of the necessary bimetallic tubes, no special requirements were imposed on the quality of 316L steel. Materials were supplied by INFN (Pisa). The materials for making tubular bimetallic samples were $\varnothing 48.26 \times 2.77$ mm tubes of GRADE 2 ASTM B 337-95 titanium (Baoji Titanium Industry Co., Ltd., China) and TP316/TP316L stainless steel (Schoeller–Bleckmann Edelstahlrohr AG, Austria), and also of BT1-0 titanium (Russia) and 12X18H10T stainless steel (Russia). Chemical compositions of the materials are given in Appendices.

The coupling was of Russian-made 12X18H10T steel, which corresponds to Western 321L steel. At VNIIEF (Sarov) they developed and implemented a method for explosion welding of coaxial pieces. For this purpose, special equipment was made. It allowed components of coaxial bimetallic joints to be welded with a necessary accuracy and minimum deviations from cylindricity caused by possible misalignment of the explosion and tube axes. For reliable and strong joining of the titanium and stainless steel components with the coupling, the power of the charge, i.e., the amount of high explosive (HE), is thoroughly

Stainless steel quality is essential

EN 1.4404 X2 Cr Ni Mo 17-12-2 (316L) • ferrite number ~ 2 • easy to procure	Tubes, bellows, fixation parts
EN 1.4435 X2 Cr Ni Mo 18-14-3 (316L also) • ferrite number ~ 0 • μr < 1.01 • less easy to procure	Tubes in cold part
EN 1.4429 X2 Cr Ni Mo 17-13-3 (316LN) μr < 1.005 • N2 enriched → hardness 150/190 HB • refined by electroslag process • forged in bars • stands baking 2 h at 950 °C • difficult to procure	CF flanges Cavity flange

Verify the real chemical composition! Standards have a wide range

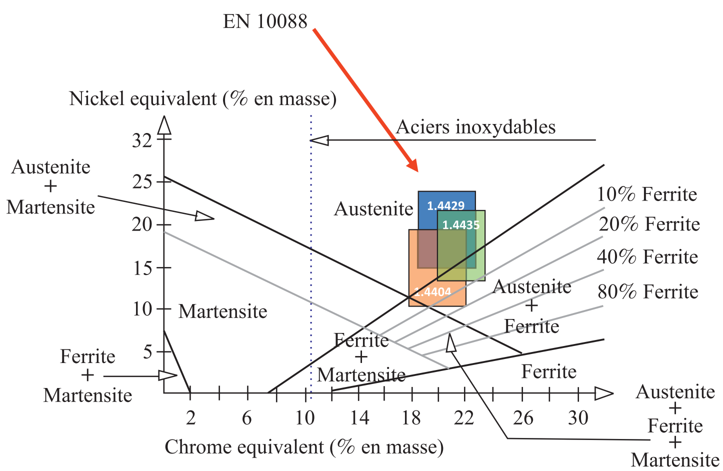

Diagramme de Shaffer

De Long model: Chrome equivalents: (Cr)eq=(%Cr)+1.5(%Si)+(%Mo)+0.5(%Nb)

Nickel equivalent: (Ni)eq=(%Ni)+0.5(%Mn)+30(%C)+30(%N)

Fig. 9. Comparative plot showing characteristics of various 316L austenitic steels

adjusted (Fig. 11). In this way, the first transition tube element with a coupling of Russian stainless steel was made (Fig. 12).

This bimetallic sample was subjected to comprehensive tests in Dubna and Pisa [6].

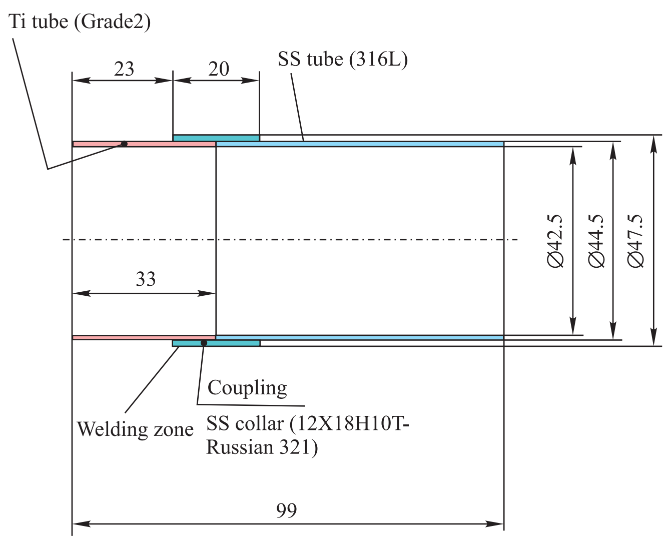

Fig. 10. Schematic view of the working version of the bimetallic tube to be made by explosion welding

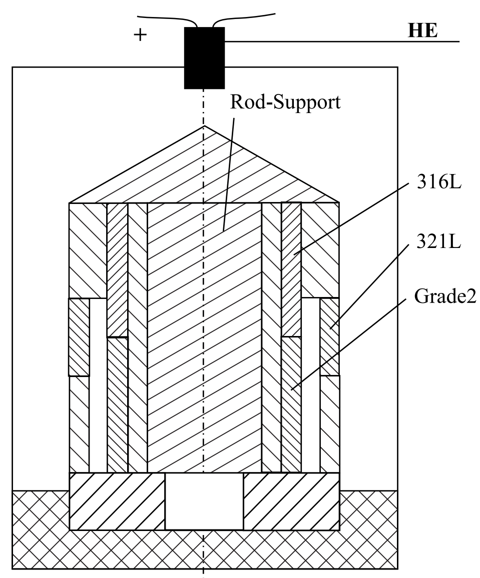

Fig. 11. Scheme of explosion welding of tubular pieces (HE means high explosive)

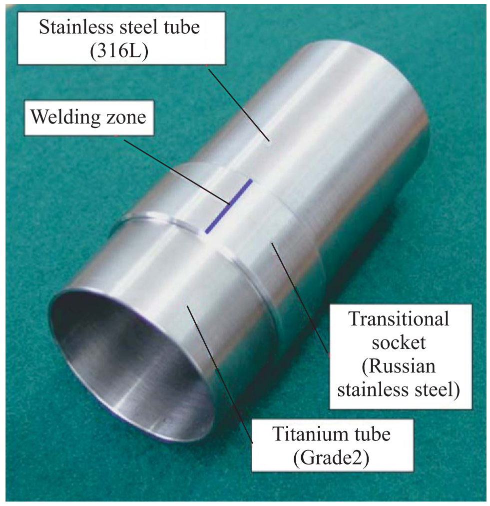

Fig. 12. Pilot welded bimetallic tube sample of Grade2 titanium and 316L steel with a coupling of Russian 12X18H10T (321L) steel

1.3. Tests of the First Ti–SS Sample at JINR, Dubna. In Dubna, the sample was put through six cycles of the thermal cycling test: cooling in liquid nitrogen (77 K) until «boiling» stopped → warming to room temperature (300 K) → cooling-down → warming-up, and so on six times. Leak measurement was performed with a PFEIFER-VACUUM HLT160 leak detector at room temperature; no leaks were found at the background leak rate $Q \leqslant 10^7$ l · atm/s after the He gas vacuum test. Then the sample was filled with helium at the pressure of 6.5 atm, the leak measurement was performed again, the leak detector showed the background leak rate $Q \leqslant 10^{10}$ mbar · l/s, and no leak was observed. Since the cryomodule will have to work at the liquid helium temperature (1–2 K), the next test was carried out at the temperature close to that of liquid helium: the sample was cooled down to $\cong$ 6 K in the cryocooler and warmed up to room temperature. The liquid helium temperature was obtained by using a shaft cryostat based on the Cryomech PT405 closed loop pulse tube refrigerator [20]. The schematic view of the cryostat is shown in Fig. 13. The cryostat allows working with samples 70 mm in diameter and 200 mm in length. The design features and performance of a similar cryostat are presented in [7]. Figure 14 shows the temperature of the sample in the cooling process. Almost the same dependence would be expected under the operating conditions of the investigated welded joint. The sample was warmed up by removing it from the cryostat. Warmed to 300 K (within approximately 1 h), the sample was inserted again in the sample chamber of the cryostat and cooled. The ultimate temperature in the

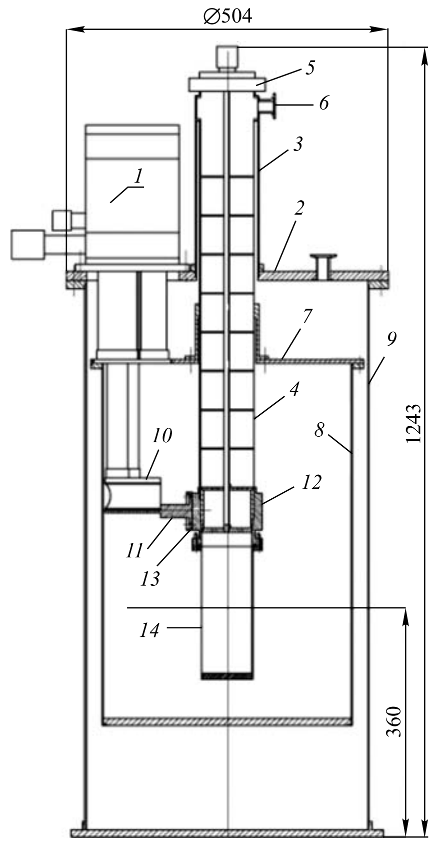

Fig. 13. Shaft cryostat based on the PT405 closed loop pulse tube refrigerator for the temperature range of 300–6 K [20]. *1* — cold head PT-405; *2* — flange of cryostat; *3* — head of cryostat; *4* — shaft; *5* — insert; *6* — flange NW25; *7* — flange cooled by first step of cold head; *8* — thermal shield; *9* — vessel of cryostat; *10* — second step of cold head; *11* — flexible thermal bridge; *12* — heat exchanger of insert; *13* — heater; *14* — sample chamber

cooling process reached 6 K during 9 hours. Six cycles like this were performed. The background leak rate measurement at room temperature yielded the value $Q \leqslant 10^{10}$ mbar · l/s, and no leak was observed.

1.4. Leak Measurement of the Ti–SS Transition Sample at INFN, Pisa. The main goal of these measurements was to evaluate the quality of the junction obtained and its stability at cryogenic temperatures. A dedicated setup was made for these tests. It consisted of a blind stainless steel flange (DN63) to close the aperture on the titanium side and a stainless steel reduction (DN63–DN25) mounted to close the stainless steel aperture from the other side.

Then a DN25 connection was mounted for the gas leak detector. Both O-rings on two flanges were made by hand using the indium wire 2 mm in diameter. The choice of this gasket was motivated by the need to carry out tests at two different temperatures: room and liquid nitrogen (300 and 77.3 K, respectively). The two standard stainless steel vacuum components (the blind

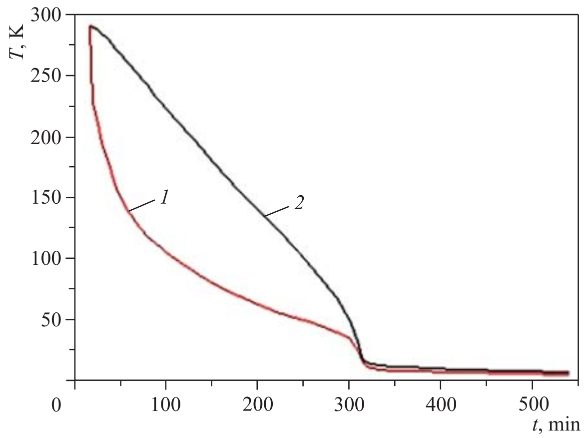

Fig. 14. Sample temperature (*2*) and the second step of the cold head (*1*) in the cooling process

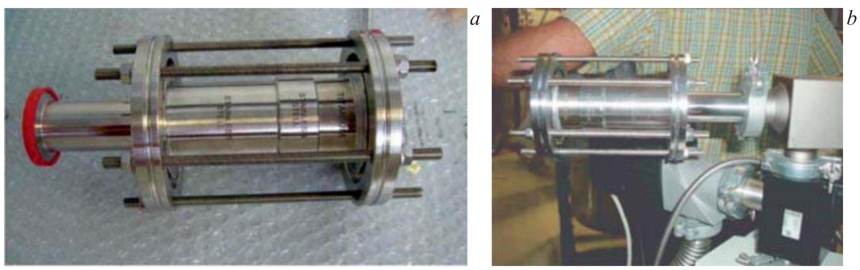

Fig. 15. Experimental setup for the Ti–SS transition sample: *a*) to be tested; *b*) connected to the leak detector with a C-clamp

flange DN63 and the DN63–DN25 reduction) and the joint sample were assembled together with six stainless steel threaded rods equipped with nuts and washers to assure appropriate vacuum seal (Fig. 15, *a*). A similar gasket (indium wire) was used for the connection between the flex pipe of the leak detector and the experimental setup. The vacuum seal was completed by using a C-clamp (Fig. 15, *b*).

The bimetallic sample was wrapped up with a plastic bag making a small volume where gaseous helium was flown for several seconds (typically 3–5 s). Figure 16 shows the measurement setup during the ongoing test at room temperature.

The measurement gave the following values:

$T = 300$ K;

vacuum level $= 5.7 \cdot 10^{-3}$ mbar;

background leak rate $= 1.2 \cdot 10^{-10}$ mbar · l/s.

Fig. 16. The Ti–SS transition sample wrapped with a plastic bag for the leak test

No changes were detected after filling the plastic bag with gaseous helium.

$T = 83$ K;

vacuum level $= 5.7 \cdot 10^{-3}$ mbar;

background leak rate $= 6.0 \cdot 10^{-9}$ mbar · l/s (at 300 K);

background leak rate $= 3.4 \cdot 10^{-9}$ mbar · l/s (at 83 K).

No changes were detected after filling the plastic bag with gaseous helium.

During the cryogenic test, temperatures were measured by two thermal diode sensors (model DT-670 produced by Lake Shore): one was attached to the sample to monitor the temperature inside the plastic bag and the other was used to monitor room temperature. In Fig. 17, we show the cool-down and warm-up temperature profiles of our sample.

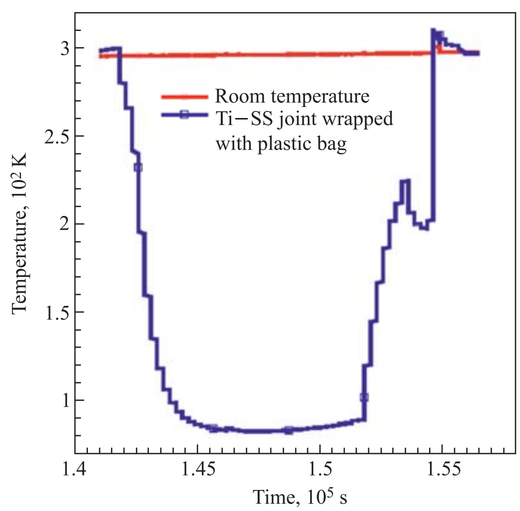

Fig. 17. (Color online). Temperatures during the leak test measurement of the Ti–SS transition sample. The room temperature is given by the red curve while the blue one represents the sample temperature

The second leak test was also performed at about 200 K (see the circle in Fig. 16). The setup was taken out of the Dewar and when the temperature reached almost 200 K, the second leak test was carried out. No variation in the background level was observed:

$T = 200$ K;

vacuum level $= 6.7 \cdot 10^{-3}$ mbar;

background leak rate $= 8.6 \cdot 10^{-9}$ mbar · l/s (at 200 K).

No changes were detected after filling the plastic bag with gaseous helium.

1.5. Leak Tests after Thermal Cycling. A deeper investigation of the Ti–SS transition sample behavior is of great importance for ILC applications considering that this part will be thermally stressed when passing, under the standard working conditions, from room temperature down to cryogenic temperatures. For these reasons it was planned to thermally stress the sample by putting it through several thermal cycles where it is cooled down from room temperature to liquid nitrogen temperature.

The same experimental setup described above (Fig. 15, *b*) without the plastic bag was used to carry out a series of leak rate and vacuum level measurements during the thermal cycles of the bimetallic sample at 300 and 77 K. At the end of the cycles, a measurement of the sample helium leak rate at room temperature was repeated. The cooling-down procedure was very quick: it took a few minutes. The sample remained in contact with liquid nitrogen in the Dewar for about 15 min (the elapsed time necessary to have the system at thermal equilibrium with LN2). The temperature of each thermal cycle was monitored by two sensors, one attached to the sample (see the blue curve in Fig. 17) and the other monitoring the room temperature (see the red curve in Fig. 17). Then the sample was taken out of the Dewar and warmed up by a heat gun for fast heating and high thermal stress. The total number of thermal cycles performed in the range from the room to liquid nitrogen temperatures was seven, as shown in Fig. 18.

At each cycle the values of the vacuum level and background leak rate both at room and at liquid nitrogen temperatures were measured. The results are summarized in Table 1.

Table 1. **Total measurements of the setup vacuum level in seven cycles**

Cycle number	Vacuum level, 10^{-3} mbar		Leak rate, 10^{-9} mbar · l/s	
	at 300 K	at 77 K	at 300 K	at 77 K
1	6.7	6.0	2.4	2.3
2	6.7	6.0	1.4	1.3
3	6.7	6.3	9.0	4.2
4	6.7	9.0	1.7	2.5
5	7.3	6.7	7.1	6.9
6	7.0	6.7	5.0	4.5
7	6.7	6.3	3.6	3.3

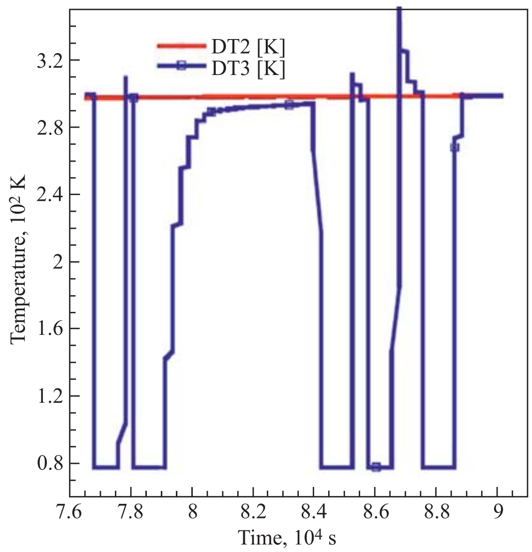

Fig. 18. (Color online). Temperature monitoring during the leak test measurement of the Ti–SS joint sample. The room temperature is given with the red curve while the blue one represents the sample temperature

It should be pointed out that between the fourth and fifth cycles, the gasket (indium wire) between the leak detector flex pipe and our sample was replaced due to vacuum tightness problem. At the end of these thermal cycles, the sample was placed again in a plastic bag and filled with gaseous helium for the vacuum level and leak rate measurements. The following results were obtained:

$T = 300$ K;

vacuum level $= 7.0 \cdot 10^{-3}$ mbar;

background leak rate $= 3.1 \cdot 10^{-9}$ mbar · l/s.

No changes were detected after filling the plastic bag with gaseous helium.

1.6. High Pressure Tests. Since the bimetallic transition sample could be used in the liquid helium distribution circuit of the ILC cryomodule, leak detection measurements of the sample were also performed at high pressure. For this purpose, the sample was connected to the helium bottle and filled with gaseous helium up to a pressure of about 6 bar (Fig. 19).

Then the sample was carefully checked for leaks by scanning the external explosion bonding joint with a probe connected to the leak detector. With this measurement technique, it is possible to localize a leaking area, but the resolution in the real leak rate is considerably worse than in the previous measurements. No leaks were found up to 10^{-7} mbar · l/s; this value is the best instrument sensitivity for this type of measurement.

Fig. 19. The sample connected to the helium bottle and filled with gaseous helium up to a pressure of about 6 bar

1.7. The Ti–SS Transition Sample with Welded Plates. In order to test the resistance of the bimetallic transition sample to TIG welding in its neighborhood, the authors processed the sample previously tested as follows: the Ti pipe was closed with a Ti plate welded to it and the stainless steel side of the joint was closed with a 3 mm thick stainless steel disk with a hole at the centre for welding a DN25 connection [6]. The technical drawing of the complete assembly is shown in Fig. 20. The welding procedure was as follows. Inside the welding box there was a container with ice and water to cool the Ti–SS sample during welding. The water-ice level was close to the welding area. The authors monitored the transition sample temperature using a probe connected to the external surface of

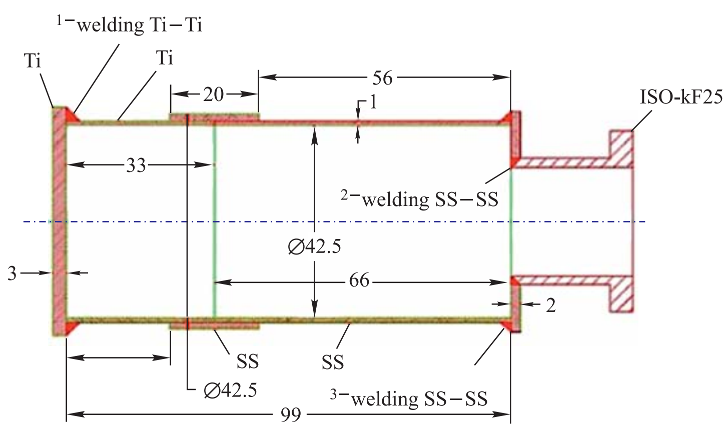

Fig. 20. Technical drawing of the Ti–SS joint with the welded components

Fig. 21. The finished welded assembly

the stainless steel collar. The welding procedure was very fast (about 5 min) and the registered temperature was always about $+3$ or $+4\,^{\circ}$C. The finished welded assembly is shown in Fig. 21. This welded part was subjected to all the tests performed before with the simple Ti–SS transition sample using the same measurement techniques:

— leak check at room temperature with a plastic bag filled with gaseous helium;

— thermal cycles between 300 and 77.3 K and, after the final (fifth) cycle, new checks for leaks at room temperature;

— leak tests under high pressure (about 6 bars of gaseous helium) inside the Ti–SS transition sample.

1.8. Results of the Leak Test at Room Temperature and after Thermal Cycling. The results of the tests at room temperature are given below:

$T = 300$ K;

vacuum level $= 6.7 \cdot 10^{-3}$ mbar;

background leak rate $= 3.4 \cdot 10^{-9}$ mbar · l/s.

No change was detected after filling the plastic bag with gaseous helium for 3–5 s.

This test procedure has already been described in Subsec. 1.2. It was repeated with the Ti–SS transition sample having the welded components. Figure 22 shows the measuring procedure. After the last thermal cycle, the sample was warmed up to room temperature with a heat gun and the vacuum level and background leak rate were measured. The results are shown below:

$T = 300$ K;

vacuum level $= 6.3 \cdot 10^{-3}$ mbar;

background leak rate $= 3.5 \cdot 10^{-10}$ mbar · l/s.

After filling the bag with the He gas we observed a significant leak. After careful study this leak was traced to a problem with the SS–SS weld. Unfortunately, this prevented the tests with this sample from being continued.

1.9. Concluding Remarks. The world's first Ti–SS transition sample has shown excellent behavior at the room, liquid nitrogen, and liquid helium tem-

Fig. 22. Thermal cycling test with the Ti–SS transition sample having the welded components — cooled sample

peratures, as well as in the high pressure and thermal cycling tests. No helium leak was detected in the sample at the background rate $\cong 10^{-10}$ mbar · l/s. The metallographic investigation proved that the joint of stainless steel and titanium is of high quality. It is a very good result for the initial tests for this type of welding, i.e., by the explosion bonding technique. To obtain more reliable data and statistics, it is necessary to perform similar tests with a larger number of samples. The experiments were continued to reach this goal.

It was also planned to install one tube (or more) on the 1.3 GHz helium vessel and test it in the Horizontal Test Cryostat at 2 K for an integrity test of only demonstration that tube can operate at 2 K after a cooldown and warm-up. The sample tested in Dubna and Pisa was presented at the Milano ILC Meeting (Autumn 2006) and made very bright impression and was highly enthusiastically approved for further production.

1.10. Ti–SS Investigation for More Statistics. After manufacturing the first Ti–SS bimetallic transition sample and getting excellent results in its tests for vacuum/pressure rate leak and mechanical behaviour, the collaboration decided to produce ten more similar samples to obtain better statistics.

At the end of January 2008, Dubna received ten transition joint samples made of Ti and SS tubes in Sarov (Russia). Two pipe sections (external diameter $1.5''$) were welded together by the explosion bonding technique applying an external stainless steel collar covering the junction line of the two materials.

The leak test measurements were performed by the Dubna–Pisa team at INFN (Pisa) using a helium mass spectrometer leak detector (model 979 by VARIAN) equipped with an internal turbomolecular high vacuum pump and a mechanical external dry scroll pump [8]. The minimum detectable leak was $< 5 \cdot 10^{-11}$ atm · cc/s. The results of the measurements are given in the next section.

1.11. The Ti–SS Transition Samples. Like the previously tested sample [4–6], ten new ones are made of two equal-diameter pipe sections, one of titanium (Ti) and the other of stainless steel (SS), connected by a SS collar explosion bonded on the external surface of the tubes (Fig. 23).

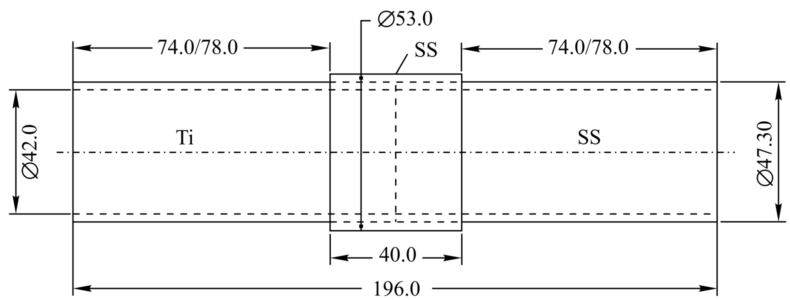

Fig. 23. Dimensions (in mm) of the Ti–SS transition samples

The pipe billets were sent to JINR from INFN (Pisa) and then redirected to RFNC, Sarov. The billets were made by cutting standard stainless steel (316L) and titanium (Gr2) seamless pipes ($1{-}1/2''$ NB × sch.10S – ISO 48.3×2.6 mm) bought from an Italian distributor but coming from Germany (SS) and China (Ti). The certificates for the materials with their chemical composition are given in Appendix 1. The SS collars were also supplied from Pisa, the material of these rings was also 316L, and they came from seamless standard pipe ($2''$ NPS x sch. 40S – ISO 60.3×3.9 mm) cutting.

It should be pointed out that all the transition joints were externally machined in Sarov after the explosion bonding process to obtain the dimensions shown in Fig. 23. All the samples (Fig. 24) were labelled on the external surface with a progressive number. Sample No. 2 was missing.

A few joints were annealed in Sarov to reduce the welding and machining stresses underwent by the sample during the explosion bonding process. As is evident from Table 2, the leak test measurements in Sarov did not reveal any difference between the annealed and nonannealed samples.

It seems today that the annealing conditions were not the best ones: the chosen temperature ($540\,^{\circ}$C) and the treatment time in a vacuum oven (about 30 min) appear to be more effective for titanium than for stainless steel [18].

Fig. 24. Photo of the nine Ti–SS samples tested in Pisa

Table 2. **Annealing process and leak rate measurements performed in Sarov**

Sample number	Annealing process	No leak detected at background, $Pa \cdot m^3/s$
1	No	$1.2 \cdot 10^{-9}$
3	No	$1.2 \cdot 10^{-9}$
4	Yes	$1.2 \cdot 10^{-8}$
5	Yes	$1.2 \cdot 10^{-8}$
6	Yes	$1.2 \cdot 10^{-8}$
7	No	$1.2 \cdot 10^{-9}$
8	Yes	$1.2 \cdot 10^{-8}$
9	Yes	$1.2 \cdot 10^{-8}$
10	No	$1.2 \cdot 10^{-9}$

The authors also think that the annealing procedure did not affect the welding joint tightness because the annealing temperature was too low for stainless steel [18].

1.12. Leak Test at Room Temperature. Each bimetallic sample was connected to the leak detector using the same setup developed to test the previous samples [6]; two blind stainless steel flanges were used to close the pipe on both sides and create a small vacuum volume. One of them was connected by a reduction joint to the flex pipe from the leak detector. A hand-made indium O-ring of the wire 2 mm in diameter was used to seal, on both sides, the vacuum volume of the joint to be tested.

The results of the test at room temperature are presented in Table 3. The measurements were performed with a plastic bag enclosing the sample filled with the He gas, as detailed in [6] and shown in Fig. 25.

Table 3. **Results of the leak test at room temperature (300 K) performed at INFN (Pisa)**

Sample number	Vacuum level, mbar	Background leak rate, atm · cc/s	He leak rate, atm · cc/s
1	< 5	0.8–1.0	No variation
3	< 5	0.1	No variation
4	< 5	4.0	No variation
5	< 5	1.2	$1.5 \cdot 10^{-10}$
6	< 5	0.9–1.0	No variation
7	< 5	0.1	No variation
8	< 5	1.5	No variation
9	< 5	0.01	No variation
10	< 5	3.2	$1.3 \cdot 10^{-8}$

Fig. 25. The Ti–SS transition joint enclosed in a plastic bag for the He leak test measurements

1.13. Leak Tests after Thermal Cycling. After the room temperature test, the sample was disconnected from the leak detector and five thermal cycles of quick passing from room temperature (300 K) to liquid nitrogen temperature (77 K) were performed for each sample.

Each sample was dipped in a Dewar filled with liquid nitrogen (Fig. 26). This cooling process was very quick because the metallic sample reached the thermal

Fig. 26. Photo of a sample dipped in liquid nitrogen within the Dewar

Fig. 27. Photo of a joint before the heating by the hot gun started

equilibrium with the liquid environment in few minutes (no bubbles were visible around the metallic surface). After that the sample was taken out of the Dewar (Fig. 27) and warmed up by a heat gun until no ice was present on the metallic surfaces (this warming procedure was also very fast).

As is mentioned above, this cooling–heating process was repeated five times for each joint before connecting it again to the leak detector for the measurement of the He leak rate at room temperature. The results of the second part of the test are presented in Table 4.

The measurements demonstrate rather stable tightness of the explosion welded Ti–SS tube joint except for tube No. 10, which shows a leak after five thermal

Table 4. **Results of the test at room temperature (300 K) after five thermal cycles**

Sample number	Vacuum level, mbar	Background leak rate, atm · cc/s	He leak rate after thermal cycles, atm · cc/s, no leak at this value
1	< 5	0.4	$0.9 \cdot 10^{-10}$
3	< 5	0.8–0.9	No variation
4	< 5	2.4–2.5	No variation
5	< 5	3.7	No variation
6	< 5	0.1	No variation
7	< 5	0.1–0.2	No variation
8	< 5	0.8–1.0	No variation
9	< 5	0.3–0.5	No variation
10	< 5	3.1	$2.1 \cdot 10^{-8}$, leak

cycles. It means that this sample has too large residual stress after explosion welding, and superposition of thermal stress on it provokes mechanical destruction in the bonding line. The total result is a 90% success.

Nine Ti–SS transition joints were characterized. Eight of them showed excellent behavior both at room temperature and after thermal cycles between room (300 K) and liquid nitrogen temperatures (77 K). The measured helium leak rates of the samples were $1 \cdot 10^{-10}$ $(\pm 10\%)$ atm · cc/s. No difference was observed in comparison with the results obtained with the annealed samples and those without any thermal treatment even if the chosen thermal treatment seemed to be more suitable as a distension treatment for the titanium material alone. Only one sample (joint No. 10) showed a small leak $(2.1 \cdot 10^{-8}$ mbar · l/s) around the collar that covered the Ti–SS junction, and this leak was present before and after the thermal cycles.

This result is very good, and we are confident that these samples can be sent to Fermilab for using them in the construction of the 3rd harmonic cavity vessels.

In 2009, more bimetallic Ti–SS tubes were made to the size complying with the specification of the IV generation cryomodule: $\varnothing_{\rm ext} = 60$ mm, wall thickness 2.5 mm, and length 170 mm. They were also put through comprehensive tests in Pisa using shock thermal cycling. Table 5 presents the results of the test for the tubes complying with the cryomodule specifications.

Table 5

Sample number	Vacuum level, 10^{-4} mbar	Background leak rate, 10^{-10} atm · cc/s (room temperature)	He leak rate, atm · cc/s (room temperature)	He leak rate after thermal cycles, atm · cc/s (room temperature)	Notes
5	< 5	3.0	No variation	No variation	OK
6	< 5	5.0	No variation	No variation	OK
9	< 5	0.5	No variation	No variation	OK
11	< 5	3.0	No variation	No variation	OK
18	< 5	0.5	No variation	No variation	OK

1.14. Cryogenic Tests of Bimetallic Tubes at FNAL. JINR, INFN, and Fermilab participate in the GDE group, the international organization that coordinates design and R&D for the ILC. In addition, JINR and Fermilab are members of the TESLA Technology Collaboration (TTC), which plays a major part in development of superconducting high-frequency technologies. This international collaboration involves contributions from many institutes, including JINR. Over the period 2006–2011, JINR has been actively cooperating with INFN, Pisa, and FNAL, Batavia, on the problem of bimetallic Ti–SS tubes connecting the titanium vessel for helium with the two-phase helium collector of the ILC cryomodule (CM). According to estimations of R. Kephart (ILC Program

Director at FNAL), these transition tubes can considerably decrease the manufacture cost of the cryomodule (even probably the IV generation cryomodule) because of replacement of the titanium tube for helium supply with the stainless steel tube.

The next step in the investigation of the properties of the samples was their testing at Fermilab at the temperature 2 K and under real cryomodule conditions. Experts of JINR and the Cryogenic Department of the Accelerator Division, FNAL, elaborated the plan and schedule of the work.

All the tubes were put through the thermal cycle test in liquid nitrogen and the vacuum test again. The results of the tests in Dubna and Pisa were confirmed: no leaks were detected under the following measurement conditions:

a) at room temperature 300 K — $7.5 \cdot 10^{-10}\,(\pm 10\%)$ Torr · l/s;

b) at the temperature 77 K — $7.5 \cdot 10^{-9}\,(\pm 10\%)$ Torr · l/s;

c) at the pressure 6.5 atm — $< 5 \cdot 10^{-10}\,(\pm 10\%)$ Torr · l/s.

Fermilab's Horizontal Test System (HTS) and Vertical Test Dewar (VTD) were used for the tests [11, 12]. The tubes were welded in pairs by their titanium ends in a special cabinet inerted with argon atmosphere (LABCONCO Glove Box) (Fig. 28). The welding procedure was as follows.

To complete the transition joint test article assembly, one Ti weld and two SS welds were required. A chamfer was machined on the Ti tubes by the Fermilab Machine Shop to facilitate the Ti welding.

Tooling was provided to support this welding job. A threaded rod with holding flanges at either end was used to hold the two transition joints together while welding. Also, water-cooled copper heat sinks were fabricated to keep the explosive-bonded joint cool during the welding process. These pieces are shown separately in Fig. 29, and installed for welding sinks are shown in Fig. 30.

Fermilab's welder performed the welds, as shown in Fig. 31.

Fig. 28. Welding the titanium ends of the transition joint test article

Fig. 29. Water-cooled copper heat sinks

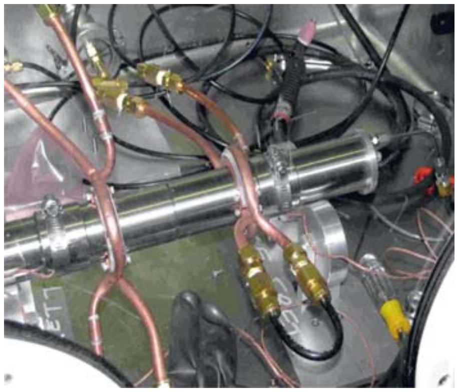

Fig. 30. The heat sinks installed for welding

Fig. 31. The transition joint test assemblies. Each has a pair of transition joints

1.15. Welding Procedure and Results. Initial testing was done with stainless steel welds to test the concept of the water-cooled heat sinks. Two stainless steel tubes were welded to imitate the welding of the bimetallic tubes. In the first case, the temperature rises from 20 to $40\,^{\circ}$C. In the second case, the temperature rise was from 19 to $30\,^{\circ}$C. This shows that the heat sinks are very effective at keeping temperatures low during the welding process.

The final production of the welding procedure for the transition joint test article assembly was carried out inside the LABCONCO Glove Box in the argon atmosphere. The following was observed:

1. The first pair to be welded is tubes 5A and 6A. Both tube pieces during welding were cooled by domestic cold water through the copper ring heat sinks fixed close to the SS collars (see Fig. 31). The temperature during the welding was measured by thermocouples on both SS collars of the pair. The elapsed time for the entire welding procedure was ~ 5 min. Temperature in °C was recorded almost every 1 min:

Left side (5A)	Right side (6A)
20.0	20.6
20.2	20.9
21.1	22.1
21.7	22.9
36.3	40.3
41.0	47.6

Around the welded line, colored spots were observed. It means that gas has admixtures.

2. The second pair consisted of bimetallic tubes 3N and 7N. They were not annealed after explosion bonding. The gas was replaced. Cooling water was flowing. Temperature measurements were performed more often:

Left side (3N)	Right side (7N)
23.6	24.0
28.1	26.6
33.6	32.7
36.7	36.1
40.1	38.8
44.2	43.4
47.7	46.9
49.6	49.9
59.9	68.2

Around the welding line, the coloration was still present, but less in comparison with the first pair.

3. The third pair included bimetallic tubes 8A and 9A, annealed after explosion welding. This pair was welded without water cooling:

Left side (8A)	Right side (9A)
23.6	24.0
28.1	26.6
33.6	32.7
36.7	36.1
40.1	38.8
44.2	43.4
47.7	46.9
49.6	49.9
59.9	68.2

The temperature increase here was not that much greater than the temperature rise for those welded with water-cooling. This suggests that these bimetallic tubes can be welded in real condition (cryomodule) without any special cooling, without any risk.

1.16. The Superfluid Test Facility. The original plans implied the use of Fermilab's Meson Detector Building Horizontal Test System (HTS) for superfluid testing of the SS–Ti transition joints.

The benefit of this installation is that the transition joints (Fig. 32) would be tested in actual service condition: superfluid He on the interior and insulating vacuum around. But a big negative factor would be the inability to get a sensitive leak-rate measurement. The HTS insulating vacuum has a relatively high He background, a relatively large volume, and much more cold connections which could be potential leak indications. These factors would make it difficult to make a straightforward leak rate assessment of the bimetallic bond. Therefore, the plans

Fig. 32. Pair of tubes connected with their titanium ends ready for tests in the horizontal test system

were altered and it was decided to test these SS–Ti transition joints in Fermilab's A0 Vertical Test Dewar (A0VTD), see Fig. 33. The major benefit of this is that the interior of the transition joint can be connected to a high vacuum Residual Gas Analyzer (RGA) for direct leak rate measurements while the exterior is bathed in superfluid. The RGA measurements will be recorded during cooldown as well. It should be noted that in this configuration, the superfluid is on the exterior side of the transition joint, opposite to the actual service conditions.

The top plate for the VTD is a new component (Fig. 34), one that has not been used before. It needs a backout to get high sensitivity/low background for

Fig. 33. A0 vertical test Dewar

Fig. 34. Transition joint test article mounted on the top insert, prior to installation in the A0VTD

initial room temperature checking. With this setup one was never able to get sensitivity better than $\sim 10^{-9}$ Torr · l/s.

Preparation for cryotemperature tests in the VTD began [11]. One by one, the tubes were connected to the high-vacuum RGA (Residual Gas Analyzer), and the leak measurement results were like previous: no leaks were identified:

a) at room temperature 300 K — $7.5 \cdot 10^{-10}$ $(\pm 10\%)$ Torr · l/s;

b) at the temperature 77 K — $7.5 \cdot 10^{-9}$ $(\pm 10\%)$ Torr · l/s;

c) at the pressure 6.5 atm — $< 5 \cdot 10^{-10}$ $(\pm 10\%)$ Torr · l/s.

Table 6 presents descriptions and sizes of the tubes welded in pairs for their tests at Fermilab under the superconducting helium conditions.

Table 6

Assembly designation	Fabrication year	Tube designation	OD, mm	Wall thick, mm	Length, mm
I	2008	5A, 6A	47	1.95	190
II	2008	8A, 9A	47	1.95	190
III	2008	3N, 7N	47	1.95	190
IV	2009	5, 6	60	2.5	170
V	2009	9, 11	60	2.5	170

Notes. The tube designations are as follows: A denotes tubes annealed after explosion welding and N denotes nonannealed tubes. The tubes without letter designations are made in 2009 to the sizes complying with the type IV cryomodule specification, nonannealed.

To prepare the tubes for further tests, they were subjected to various kinds of cleaning, including ultrasonic one. There are different opinions as to the effect of ultrasonic exposure of the weld area: (i) welding residual stress is relieved in the material junction area; (ii) the microstructure of the weld (50 to 100 μm thick) is destroyed, which leads to a decrease in the junction strength. Therefore, it would be interesting to check it in the experiments with the tubes made in 2009. One of the tested tubes was exposed to ultrasound in a mode normally used at Fermilab for ultrasonic cleaning of articles to be used in a superconducting cavity operating with a gigahertz frequency, i.e., the article was exposed to ultrasound for half an hour while immersed in water at room temperature. The next tube was exposed to ultrasound for an hour under the identical conditions. The third tube was immersed into hot water (100 °C) and was exposed to ultrasound for half an hour. Then all the tubes were leak-checked at room temperature; there were no leaks at the same level of $7.5 \cdot 10^{10}$ $(\pm 10\%)$ Torr · l/s (measurements were performed at the VARIAN leak detector).

Thus, tubes 5, 6, 9, and 11 were exposed to ultrasound in Pisa; and tubes 5A, 6A, 8A, and 9A, at Fermilab.

The thus produced tube pairs were connected to the high-vacuum RGA (Residual Gas Analyzer) for the initial quick test after the ultrasonic exposure to the Ti–SS joint. The results of the test are presented in Table 7.

Table 7

Assembly designation	He leak rate at ambient temp. and 77 K, initial, $Pa \cdot m^3/s$	He leak rate at ambient temp. after ultrasonic cleaning, $Pa \cdot m^3/s$	Comment	Tube with leak
I	< 5	$< 5 \cdot 10^{-11}$	OK, no leak	None
II	< 5	$\sim 1 \cdot 10^{-7}$	Leak	8A
III	< 5	$\sim 5 \cdot 10^{-11}$	OK, no leak	7N
IV	< 3	$< 3 \cdot 10^{-13}$	OK, no leak	None
V	< 3	$< 4 \cdot 10^{-13}$	OK, no leak	None

As is evident from the table, an obvious leak was identified in pair II, tube 8A (Fig. 35). In tube 7N the leak increased within $< 10\%$, which can be ignored. There are no grounds to state that the leak in tube 8A is uniquely due to ultrasonic exposure because other tubes made by the same explosion welding method and passed through thermal cycling, pressure, and Ti–Ti welding tests do not react in any way to ultrasonic exposure. Yet, the fact is that the leak occurred after ultrasonic cleaning.

Fig. 35. Arrow points to the place where the leak occurred in tube 8A, which is the titanium–collar joint

Tube tests at the superfluid helium temperature (2 K) were carried out in two setups, the Vertical Test Dewar (VTD) and the Horizontal Test System (HTS).

For the VTD testing, the tube pair was connected to the RGA, pumped out, and immersed in superfluid helium. In the HTS, the transition elements are tested under real superfluid helium conditions with insulating vacuum around them. The results of the tests are presented in Table 8.

The tube pair 5P and 6P was tested in the VTD twice for a short time (0.3 and 1.5 h) and in the HTS for 30 h. The measurements gave stable results: no leak at the background of $\cong (2-3) \cdot 10^{-11}$ $Pa \cdot m^3/s$.

The tube pair 9 and 11 from the last batch of the tubes with a changed size was tested in the VTD for 23 h; the tube pair 5 and 6, for 20 h. The result was also quite impressive: no leak was observed at the background of $\sim 10^{-12}$ $Pa \cdot m^3/s$ [12, 13]. Figure 36 shows the results of the 16-h-long leak measurements for the pair 5P and 6P in the HTS on 15–16 January 2009. It is evident from the figure that no leak was observed in the joint kept within 16 h at 2 K.

Table 8. **Results of bimetallic transition assemblies leak measurements under superfluid conditions**

Assembly designation	Test system	Initial leak rate, ambient, $Pa \cdot m^3/s$	Duration of 2 K conditions, h	He leak rate, superfluid, $Pa \cdot m^3/s$	Final He, leak rate ambient, $Pa \cdot m^3/s$	Conclusion
I	A0 VTD	$< 5 \cdot 10^{-10}$	0.3	$< 5 \cdot 10^{-10}$	$< 2 \cdot 10^{-11}$	No leak observed
I	MDB HTS	$< 7 \cdot 10^{-11}$	30	$< 3 \cdot 10^{-11}$	$< 3 \cdot 10^{-11}$	No leak observed
I	A0 VTD	$< 6 \cdot 10^{-13}$	1.5	$< 6 \cdot 10^{-13}$	$< 10^{-12}$	No leak observed
V	A0 VTD	$< 5 \cdot 10^{-13}$	23	$< 3 \cdot 10^{-11}$	$< 10^{-12}$	No leak observed
IV	A0 VTD	$< 7 \cdot 10^{-13}$	20	$< 8 \cdot 10^{-11}$	—	No leak observed

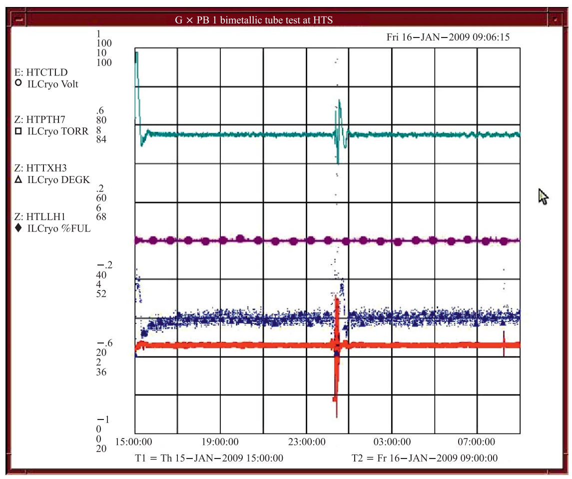

Fig. 36. (Color online). RGA readings at test of the tube pair 5A + 6A in the HTS. Lilac points are the leak detector readings. Curves are the liquid helium level (green), leak detector readings (lilac), helium temperature (blue), and helium pressure (red)

1.17. Conclusion. Properties of explosion-welded bimetallic Ti–SS transition elements intended for IV generation modules of the ILC have been investigated. A unique technology for explosion welding of tubular pieces from dissimilar materials is described and the results obtained in investigations of the physical and mechanical properties of the produced articles and in their cryogenic tests are presented. Nine bimetallic tubes with the external diameter 47 mm, length 190 mm, and walls 1.95 mm thick and five tubes with the external diameter

60 mm, length 179 mm, and walls 2.5 mm thick were used in the tests. The test procedure included the following.

1. Macroanalysis.

2. Microanalysis.

3. Mechanical strength tests of the joints.

4. Thermal cycle tests to 77 K and leak measurement at liquid nitrogen temperature and room temperature and at high vacuum of 10^{-4} Torr.

5. Pressurization of the tubes to 6.5 atm and leak rate measurement at room temperature.

6. Exposure of the articles to ultrasound under different conditions and leak measurements at room temperature.

7. Leak-checking at the liquid helium temperature of 1.8 K.

The results of the investigations have shown that the Ti–SS explosion welding makes reliable and strong joining and that the shear strength is $\cong$ 250 MPa. The joint is highly leak-proof: the average leak rate was no higher than 10^{11} Pa $\cdot$ m^3/s.

At the end of 2008, Siemens published a calendar for 2009. Each page of the calendar presented one of 12 outstanding world technology achievements in 2008. The opening January page showed an artist's view of the cryomodule developed at the Fermi National Accelerator Laboratory (FNAL) for the future International Linear Collider (ILC) (Fig. 37). One of the components of this complex device is the explosion-welded Ti–SS transition element made by the JINR–VNIIEF–FNAL–INFN collaboration, which connects the helium vessel to the two-phase liquid helium supply pipe running along the entire 35-km-long ILC.

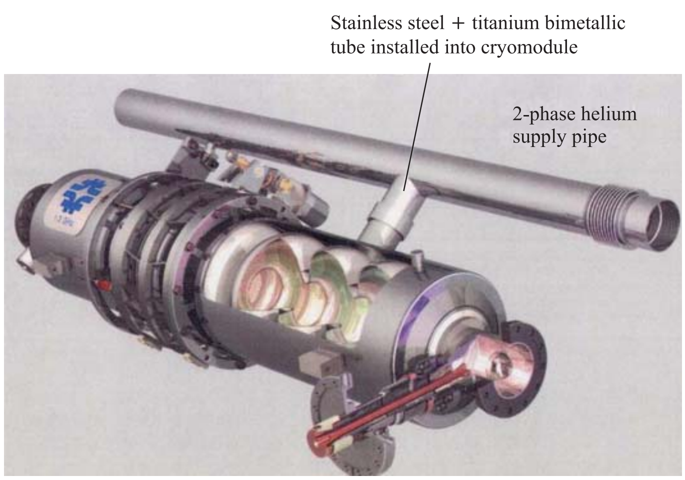

Fig. 37. Cryomodule with the built-in Ti–SS transition element

2. REDESIGNING OF THE IV GENERATION CRYOMODULE FOR THE ILC

2.1. Development of the Technology for Production of Nb–SS Transition Elements. The results obtained in explosion welding of bimetallic Ti–SS tube pieces allowed the collaboration to set about solving a much more complicated problem of the redesigning of the IV generation cryomodule by replacing titanium with stainless steel as the material for the helium Dewar shell. The new design would considerably facilitate the construction of the cryomodule and, which is most important, would substantially reduce the cost of the accelerator. It should be borne in mind, however, that the steel to be used for the new Dewar shell had to have minimum residual magnetism [17]. According to the specification, only austenitic 316L steel can be used for the cryomodule. In particular, it should be EN 1.4429 (316LN) steel, which, as is evident from the plot in Fig. 9, has a minimum ferrite component admixture ($< 5\%$) and no martensite component at all.

Since our task was to develop the welding technology and the design for the needed bimetallic transition elements, no special requirements were placed on the 316L steel quality.

The common JINR–VNIIEF–FNAL–INFN discussions resulted in working out two schemes of making a transition element between the niobium cavity and the steel shell (Fig. 38).

After the design of the Nb–SS transition elements was in general agreed upon, working drawings of the transition elements to be fabricated by the two welding schemes were made at Fermilab under constant supervision of JINR (Fig. 39).

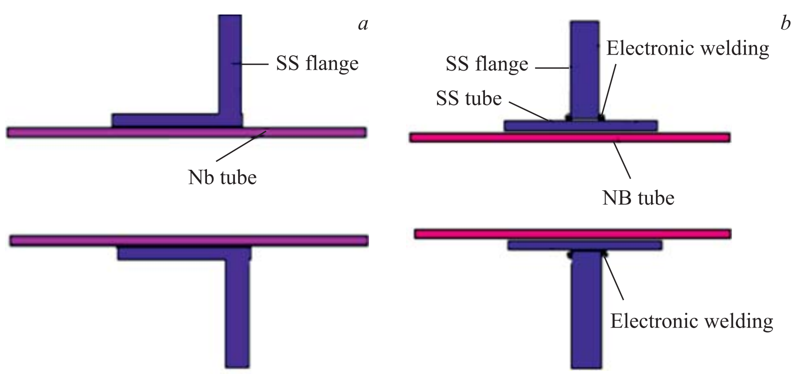

Fig. 38. Two schemes of making Nb–SS transition elements through explosion bonding of a niobium tube and a stainless steel flange: *a*) the niobium tube is welded directly to the SS flange from inside by the internal explosion in the tube; *b*) the stainless steel tube is welded to the niobium tube by the external explosion and then the flange is welded to it by electron-beam welding

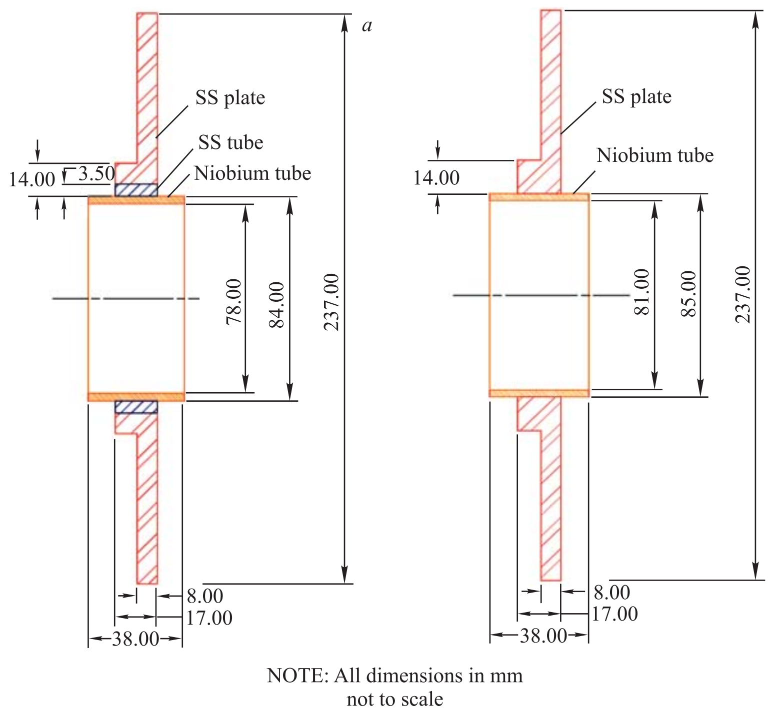

Fig. 39. Working drawings for fabrication of the Nb–SS transitions from the niobium cavity to the stainless steel Dewar shell in two versions: *a*) external explosion cladding and *b*) internal explosion cladding

Fabrication of Nb + SS transition elements by the internal explosion cladding (plot *b*) appears to be more preferable because it is an easier-to-implement, simpler, and cheaper process.

2.2. Fabrication and Tests of the First Pilot Nb–SS Transition Elements. Four pilot Nb–SS transition joints, two of each of the two explosion welding versions, were made and experimentally investigated in Sarov. Figure 40 shows one of them made by the internal explosion cladding.

Also, preliminary leak checks, macroanalysis and microanalysis of the pilot joints were carried out in Sarov. The results of the analyses allow the conclusion to be drawn that niobium and stainless steel were quite successfully joined:

— No leak was observed (room temperature measurement) at the background leak rate $\cong 10^{-9}$ atm $\cdot$ cm$^3 \cdot$ s^{-1} in all test articles.

— Metallographic analysis did not reveal any deviations from the structure of the welded components.

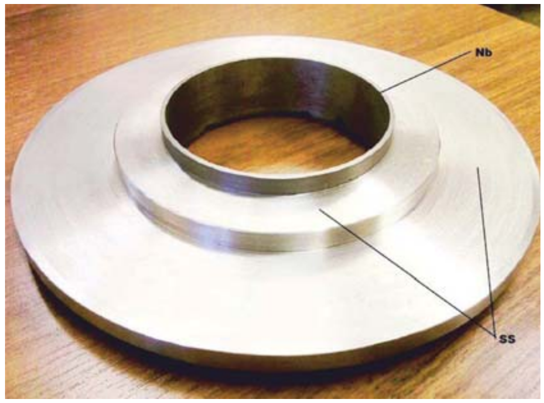

Fig. 40. World's first Nb–SS transition joint made by the explosion welding (internal explosion cladding)

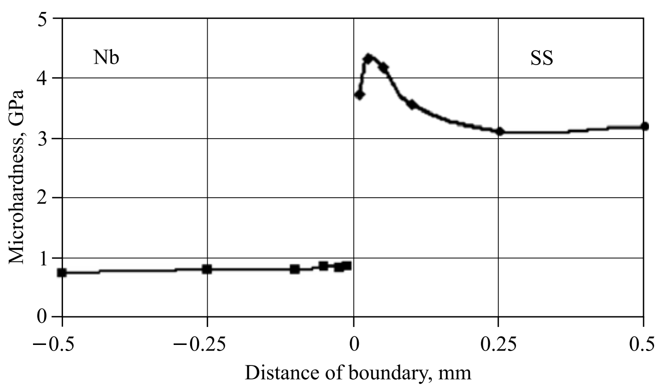

Fig. 41. Typical microhardness distribution in the zone of the niobium–stainless steel joint produced by explosion welding

— In the narrow Nb–SS contact zone 0.2–0.25 mm wide microhardness $\cong 4.4$ GPa is formed (Fig. 41).

2.3. Tests of the Nb–SS Joints at INFN, Pisa, Italy. At INFN (Pisa) the transition joints were tested under extreme conditions of thermal cycling in liquid nitrogen and ultrasonic exposure. Special equipment was made for these tests at INFN (Fig. 42). It allows one end of the transition element to be tightly sealed with indium gaskets and the other end to be connected to the vacuum pump and the leak detector.

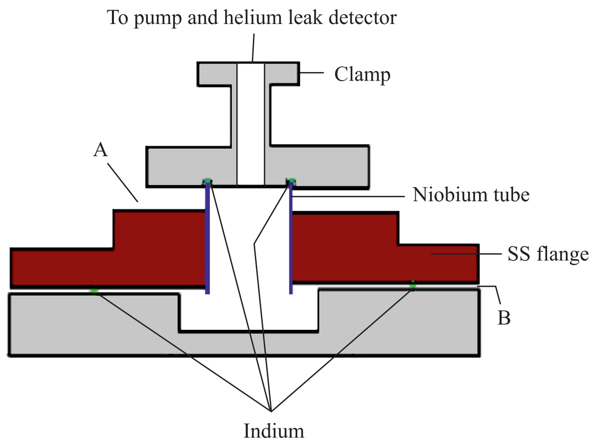

Fig. 42. Experimental layout for leak checking of Nb–SS transitions

Fig. 43. Pumped-out assembly is placed in a plastic bag and the He gas is being blown in

The leak measurements were performed in the same way as with Ti–SS tubes: the assembly was pumped out to the vacuum of 10^{-4} Torr and the background leak was measured; then the assembly was placed in a plastic bag and the He gas was blown in through a thin pipe (Fig. 43).

For technical reasons, only the upper limit of the leak rate at the nitrogen temperature could be found for all joints. It was $\leqslant (3\text{–}5) \cdot 10^{-10}$ atm $\cdot$ cm$^3 \cdot$ s^{-1}. Further investigations were carried out at Fermilab's cryogenic installation VTD.

2.4. Cryogenic Tests at Fermilab. The key problem to solve was finding out whether the Nb–SS transition elements made by explosion welding at VNIIEF (Sarov) can be used in the IV generation cryomodules of the ILC. First of all, test rigging was made for connection of the sealed bimetallic article to the vacuum system and the Residual Gas Analyzer (RGA) at Fermilab's experimental hall A0 (Fig. 44).

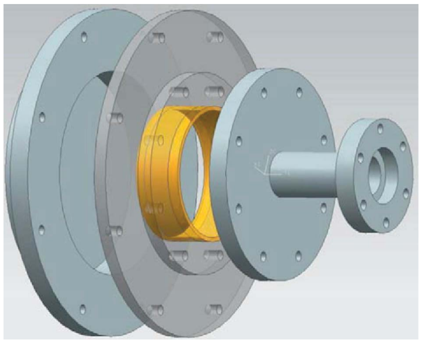

Fig. 44. Test rigging for tests of Nb–SS joints

Fig. 45. Nb–SS transition joint with the identified leak points

The thermal cycle test to the liquid nitrogen temperature carried out for leak-checking of Nb–SS steel joint 5 made by the internal explosion cladding gave a good result: after six thermal cycles and ultrasonic cleaning no leak was observed in the joint at the leak detector background reading $2{\cdot}10^{-9}$ atm $\cdot$ cm$^3 \cdot$ s^{-1} (gaseous He was used for vacuum testing).

The decisive test was the test for resistance of the welded joint to the high temperature during the welding of the niobium tube of the Nb–SS transition element to the niobium cavity. The niobium melting point is $2460\,^{\circ}$C. Niobium rings of the size matching the size of the niobium tube in the transition element were made in Dubna for this test. The rings were welded to both sides of the tube by electron-beam welding at the Sciaky Company (Chicago). The very first leak check at room temperature revealed a large leak in one of the four joints at two points in the Nb–SS steel bonding line. The holes were stopped with the Apiezon-Q vacuum paste, and the test was continued in the thermal cycling mode. After the third cycle another leak was identified, and the test was stopped. Figure 45 shows the joint with black arrows indicating the leak points.

Thus, it was demonstrated that high temperature greatly affected leak-proofness of the joint produced by explosion welding. The problem seemed to arise from structural changes in the materials caused by the explosion welding process and thermal load. Appropriate investigations were carried out with the neutron beams at PSI (Zurich), and the results are presented in Subsec. 2.5.

Since two more Nb–SS transition joints were left (articles 1 and 2 made by the external explosion cladding), it was decided to anneal them for relieving residual stresses both before and after the electron-beam welding procedure. The annealing process was agreed upon with the leading expert in materials science at Fermilab Lance Cooley [18]: heating in vacuum at a rate of $3\,^{\circ}$C/min to $750\,^{\circ}$C, maintaining for 120 min at this temperature, and natural cooling-down in vacuum in the switched-off oven. When cooled down, the joints were subjected to ultrasonic cleaning in a 2% solution of the Micro90 agent in deionized water at room temperature for 30 min, washed in isopropyl alcohol, and left to dry in the clean room for a night.

As was mentioned in Subsec. 1.16, in the literature there are different opinions as to the effect of the ultrasonic cleaning: (i) ultrasound destroys the welded joint;

Table 9. **The results of measurements in one of the cycles**

Parameters	Test article 1	Test article 2
Background leak at room temperature, atm · cc/s	$1.0 \cdot 10^{-9}$	$5.3 \cdot 10^{-9}$
Background at 77 K, atm · cc/s leak	No change	No change
Test article in polyethylene bag, gaseous He injected, 77 K, atm · cc/s	$1.2 \cdot 10^{-9}$	$5.0 \cdot 10^{-9}$
Test article warmed up to room temperature, gaseous He injected, atm · cc/s	No change	$4.9 \cdot 10^{-9}$

Fig. 46. Test article 2 ready for insertion into the VTD

(ii) ultrasound relieves internal residual stresses. The latter appears to be more reliable, which follows from the experience of the authors in ultrasound cleaning of previous $\mathrm{Ti} + \mathrm{SS}$ joint without any negative consequences.

The test articles were leak-checked through the thermal cycle test using the Dupont (Ametek upgrade) leak detector with the sensitivity 10^{-10} atm · cc/s for test article 1 and 10^{-11} atm · cc/s for test article 2. The detector was calibrated using an article with a standard leak of $5.3 \cdot 10^{-8}$ atm · cc/s. Six thermal cycles were carried out. The results of the measurements showed minimum deviations from cycle to cycle. In all thermal cycles, no leak was observed in any of the transition joint test articles.

Next was the test at helium temperature 2 K. The transition joint test article was fixed to a special rig to be inserted into the Vertical Test Dewar (VTD) with liquid helium (Fig. 46). In the figure, one can see cables running from the temperature sensors attached to the $\mathrm{Nb} + \mathrm{SS}$ test article at its top, bottom, and side. The cooling-down process lasts from 15 to 20 h with liquid nitrogen, supply of two-phase helium and cooling down to 4 K, and finally pumping-out with helium turning into the superfluid state at 1.6–2 K. Leak and temperature of the test articles were constantly measured at all cooling-down stages.

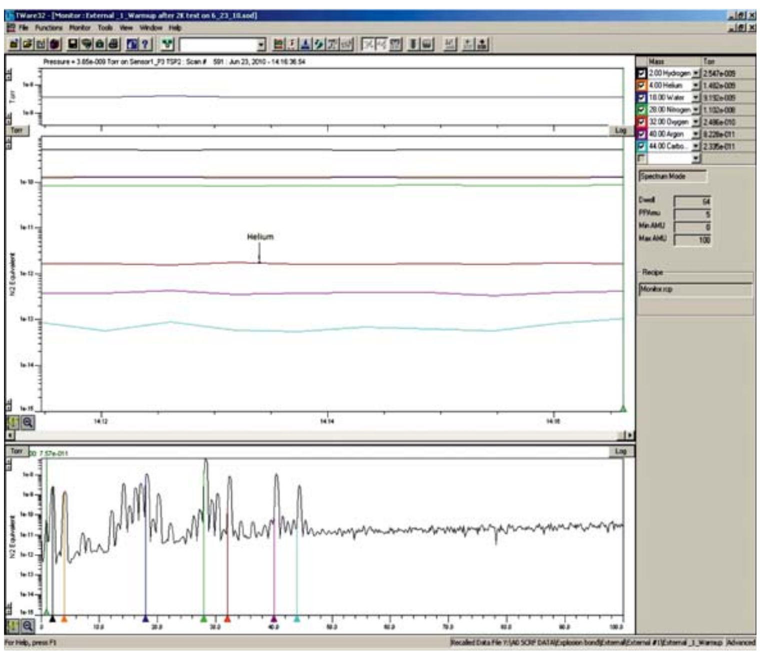

Fig. 47. Leak-level measurement histogram for test article 2

Figure 47 shows the mass distributions of the gases remaining after the pumping-out to the vacuum of 10^{-9} Torr which were measured using the Residual Gas Analyzer (RGA). The data are for the 1-h-long exposure of test article 2 at the temperature 2 K. The measured background with no leak observed during the 1-h-long exposure was $4.57 \cdot 10^{-9}$ atm · cc/s. The test with the other joint at 2 K also revealed no leak at the background $4.6 \cdot 10^{-9}$ atm · cc/s.

2.5. Neutron-Diffraction Investigation of Internal Residual Stresses Resulting from Explosion Welding. It is well known that many production processes like machining, forging, stamping, rolling, welding, etc., can result in a strong field of residual mechanical internal stresses in the material or product due to its plastic deformation. Residual stresses are often inhomogeneous and, as a rule, unpredictable. Destruction of mechanical components or structures is a consequence of not only stresses arising while those components and structures are in use but also superposition of the latter stresses on residual stresses. Tensile residual stresses can be combined with the in-use loads, which can result in destruction. To solve the problem, we have to (i) find out how high the internal residual stresses are and (ii) find the way to relieve the stresses.

Residual stresses are traditionally measured by mechanical, physicotechnical, and diffraction methods. These methods are grouped into three basic categories: (1) destructive, (2) semidestructive, and (3) nondestructive. Destructive and semidestructive methods involve only a few nonrepeatable measurements, and thus the residual stress calculations can be doubtful for all samples. Nondestructive physicotechnical methods using ultrasonic or magnetic instruments are quicker to perform measurements but, being semiquantitative, strongly depend on the material. As to the traditional X-ray diffraction method, it is limited to surface measurements because of strong absorption in most materials. Neutrons as a probe of the atomic structure have a substantial advantage over X-rays and electrons. Unlike X-rays and electrons, which interact with electron shells, neutrons interact with atomic nuclei, which allows their diffraction. Neutrons are weakly absorbed by materials, which makes it possible to perform nondestructive measurement of deformation deep in the articles. Several international and national scientific centers have built neutron diffraction facilities for a wide range of research.

We decided to measure residual stresses in Ti–SS tubes using the neutron diffraction method. The choice of the titanium-to-stainless steel joint was dictated by both the technical requirements and the availability of the materials for the experiment. We proceeded from the fact that the welding process is identical for Ti–SS and Nb–SS joints and thus the physics of diffusion of materials and occurrence of residual stresses in the joint should also be identical. Measurements were carried out with the POLDI stress diffractometer on the neutron beam from the ISIS reactor of the Paul Scherrer Institute (Switzerland) [16]. Omitting the details of the measurements and the calculation technique, we only give the

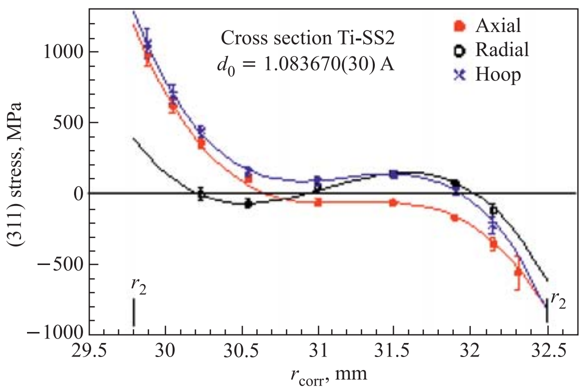

Fig. 48. Measured (points) and fitted (curves) radial dependences of the stress tensor components obtained for the peak (311) in the Ti–SS cross section

ultimate result of residual stress measurements in the bimetallic Ti–SS tube in the process of scanning the titanium-to-stainless steel joint (Fig. 48).

As is evident from the plot, the residual stress is quite considerable, amounting to ≈ 1000 MPa. Considering that additional thermal loads may arise from the electron-beam welding or the deep cooling in liquid helium, their superposition can make titanium turn into the state which corresponds to the deep plastic region. This may cause local microcracks in the Ti–SS (or Nb–SS) joint, which in turn may adversely affect tightness of the transition element when it is used in the cryomodule.

2.6. Concluding Remarks

1. It is shown that residual stresses arising from the explosion welding of dissimilar materials (Ti, Nb–SS) are rather high, which, with superposition of thermal residual stresses inside the joint region, causes plastic deformation and destruction of the bonding of the materials.

2. Annealing of explosion-welded Nb–SS transition elements before joining them with the niobium tube of the cryomodule and after their electron-beam welding completely relieve internal stresses in Nb–SS joints and makes the transition elements serviceable.

3. The thermal cycle tests with LN2 and the tests at 2 K carried out after the relieving procedures showed excellent results: no leak was observed in test articles 1 and 2 made by the external explosion cladding process at the background leak rate $\approx 4.6 \cdot 10^{-9}$ atm · cc/s.

3. SUMMARY

The main result of the joint R&D accomplished by the JINR–VNIIEF–FNAL–INFN Collaboration in 2006–2011 is the fabrication of bimetallic articles by the explosion welding method, which, as the tests showed, proves that it is quite possibe for the cavity and the helium vessel of the IV generation cryomodule in the International Linear Collider (ILC) to join.

It is shown that the residual stresses arising from the explosion welding can be relieved by annealing, which makes the transition elements quite serviceable. The thermal cycle tests with LN2 and the tests at 2 K were carried out after the relieving procedures had shown excellent results: no leaking was observed in the test articles at the background leak rate $\approx 4.6 \cdot 10^{-9}$ atm · cc/s [19].

Thus, the results of the investigations have shown that explosion welding of such dissimilar materials like titanium and stainless steel in the tubular form and niobium and stainless steel allows the joints to meet high requirements of service under extremely difficult conditions of the ILC cryomodule (Fig. 38).

The developed explosion welding procedure for bonding dissimilar materials in the tubular form can be applied to any structures where this kind of joint is needed.

Acknowledgements. We would like to gratefully acknowledge and extend our great appreciation to our co-authors A. Balagurov, A. Chernikov, Y. Taran from JINR, FLNP (Dubna, Russia); A. Venter from PSI (Switzerland); I. Malkov, V. Perevozchikov, V. Rybakov, Ju. Samarokov, and V. Zhigalov from RFNC–VNIIEF (Sarov, Russia); N. Dhanaraj, M. Foley, E. Harms, R. Kephart, A. Klebaner, D. Mitchell, S. Nagaitsev, and W. Soyars from FNAL (Batavia, USA), and A. Basti, F. Bedeschi, F. Frasconi, and S. Linari from INFN (Pisa, Italy) for their invaluable contribution into the current tests and publications in the course of works.

We express our thanks to the personnel of the Cryogenic Department of the Accelerator and Technical Divisions of FNAL K. A. Anderson, H. Carter, L. Cooley, M. McGee, R. Montier, W. Muranie, D. Plant, B. Smith, B. Tennis, and V. Yarba for the organization and technical assistance in the preparation and conducting of the tests, as well as to the technical personnel of the INFN for production of the testing facility and assistance in the conducting of the tests in Pisa.

We would like to express our special gratitude to the technical personnel of the RFNC–VNIIEF for their fruitful creative work on the development of the unique bimetallic pipe joints.

We also appreciate and are deeply grateful to the former Director of the JINR, Academician A. N. Sissakian, and the scientific supervisor from the RFNC–VNIIEF Academician R. I. Ilkaev, for their farsighted initiative, which had given the start to the quite perspective direction in research of application of the welding-by-explosion method to the modernization of the cryosystem of the International Linear Collider (ILC). The success in the fore-mentioned research was possible to achieve only under their ongoing support.

APPENDIX

Table 10. **Chemical composition of titanium (%)**

Grade	Fe	C	N	O	H	Impurities		Ti	Source
						Each	Total		
GRADE 2	0.14	0.01	0.019	0.13	0.004	< 0.1	< 0.4	Base	Certificate No. C200325024-1 of 03.03.2003
BT1-0	$\leqslant 0.25$	$\leqslant 0.07$	$\leqslant 0.04$	$\leqslant 0.2$	$\leqslant 0.01$	—	$\leqslant 0.3$	Base	GOST 19807-91

Table 11. **Chemical composition of stainless steel (%)**

Quality	C	Si	Mn	P	S	Cr	Mo	Ni	B	Fe	Source
TP316/ TP316L	0.008	0.35	1.53	0.022	0.007	16.94	2.03	11.14	0.0008	Base	Certificate No. 110819 of 31.05.2006
12X18H10T	$\leqslant 0.12$	$\leqslant 0.8$	$\leqslant 2.0$	$\leqslant 0.035$	$\leqslant 0.03$	17–19	—	9–11	Ti 5· C-0.8	Base	GOST 5632-72

REFERENCES

1. *Tsuchiya K. et al.* KEK, Tsukuba, Ibaraki, 305-0801, Japan.
2. Explosive Pipe Coupling Method. US Patent 3.710.434. 1973;
   Method for Producing Composite Metallic Pipe by Pressure Welding. US Patent 3.740.826. 1973;
   Konon Yu., Pervukhin L., Chudnovski A. Explosion Welding. M.: Mashinostroenie, 1987.
3. *Szymlek K.* Review of Titanium and Steel Welding Methods // Ship Materials, Corrosion and Environment Protection Division. Gdansk, Poland. DOI:10,2478/v10077-008-0023-4.
4. *Malkov I. et al.* Investigation of the Possibility of Production of the Bimetallic Tube Transition Element by Explosion Welding for the Cryomodule of the International Linear Collider. JINR Commun. E13-2008-109. Dubna, 2008.
5. *Sabirov B.* Production of Bimetallic Transition Tube Elements for the ILC Cryomodule // JINR News. 2008. No. 4. P. 19.
6. *Basti A. et al.* Leak Rate Measurements on Bimetallic Transition Samples for ILC Cryomodules. ILC-REP-PIS-002. 2007; JINR Commun. E13-2008-110. Dubna, 2008.
7. *Chernikov A. N. et al.* Shaft Cryostat on the Basis of Closed-Circuit Refrigerator for Neutron Powder Diffraction Studies in the Temperature Range 6–300 K. JINR Commun. P8-2005-23. Dubna, 2005 (in Russian).
8. *Basti A. et al.* Characterization Measurements of Ti–SS Bimetallic Transition Joint Samples. ILC-NOTE-2008-044. 2008; JINR Commun. E13-2008-111. Dubna, 2008.

9. *Valentini R. et al.* Microstructural and Qualitative Chemical Analysis of a SS–Ti Transition Joint Obtained by Explosion Bonding Technique. Laboratorio di Scienca dei Metalli. Univ. di Pisa, 2007.
10. *Basti A. et al.* Mechanical Tests of Titanium–Stainless Steel Bimetallic Transition Joints. ILC-NOTE-2008-046.
11. *Ghosh M., Chatterjee S.* Diffusion Bonded Transition Joints of Titanium to Stainless Steel with Improved Properties // Mat. Sci. Eng. A. 2003. V. 358. P. 152–158.
12. *Soyars W. et al.* Superconducting Radiofrequency Modules Test Facility // Advances in Cryogenics Engineering. Melville, New York: Am. Inst. of Physics, 2008. V. 53. P. 133.
13. *Budagov J. et al.* Superfluid He Testing of Stainless Steel–Titanium Transitions Fabricated by Explosive Welding. JINR Commun. E13-2009-99. Dubna, 2009.
14. *Soyars W. et al.* Superfluid Helium Testing of a Stainless Steel to Titanium Piping Transition Joint // Cryogenic Engineering Conf. Tuscon, Arizona, USA, 2009.
15. *Sabirov B.* Explosion Welding: New Design of the ILC Cryomodule // JINR News. 2010. No. 3. P. 16.
16. *Taran Yu.V. et al.* Residual Stresses in an Explosion Welding Titanium–Steel Bilayer Pipe by Neutron Diffraction // JINR News. 2011. No. 4. P. 16.
17. *Prat S.* XFEL Coupler: Industrial Assessment and Industrialization // SCRF Meeting, Fermilab, Batavia, USA, April 21–25, 2008.
18. *Cooley L.* FNAL. Technical Division. Batavia, USA, 2011. Private Communication.
19. *Sabirov B.* Recent Advances in Ti and Nb Explosion Welding with Stainless Steel for 2 K Operating (ILC Program) // Proc. of the Intern. Workshop on Future Linear Colliders (LCWS11), Granada, Spain, Sept. 26–30, 2011; arXiv:1201.3472.
20. *Budagov J. et al.* Leak Rate Measurements on Bimetallic Transition Samples for ILC Cryomodules. JINR Commun. E13-2008-110. Dubna, 2008.